https://doi.org/10.5194/egusphere-2026-1044
Preprint. Discussion started: 28 May 2026


# Redistribution of frost weathering across Spain under recent climate warming

Carlos Gabriel Morales[1], María Teresa Ortega[1], Javier Martínez-Martínez[2,*]

[1] Geography Department. University of Valladolid. Campus Sq. 47011 Valladolid, Spain

[2] Instituto Geológico y Minero de España, Consejo Superior de Investigaciones Científicas (IGME-CSIC), La Calera 1, Tres Cantos, Madrid 28760, Spain

* Corresponding autor: Javier.martinez@igme.es

**Abstract.** Frost weathering (cryoclasty) is a key cryospheric process controlling rock breakdown, sediment production, and the mechanical evolution of landscapes at mid- to high latitudes. Its effectiveness depends on the interaction between temperature variability, moisture availability, and the frequency of freeze–thaw transitions. Here we analyse the spatial and temporal dynamics of frost activity across Spain during 1993–2022 using daily temperature and precipitation records from 84 meteorological stations spanning alpine, oceanic, inland Mediterranean, coastal, and subtropical environments. Five cryoclimatic indicators were evaluated to characterise both thermal severity and hydro-thermal effectiveness: Frost Days (FD), Freeze–Thaw Cycles (FTC), Intense Freeze–Thaw Cycles (IFTC), the Frost Intensity Index (FI), and the Wet-Frost Index (WFI).

Results reveal a strong concentration of effective frost weathering in mountainous and perimountainous regions, while frost activity is marginal or absent in lowland Mediterranean, coastal, and subtropical areas. Over the last three decades, most of Spain shows a statistically significant decline in frost days and freeze–thaw cycles, accompanied by a shortening of the frost season. In contrast, peri-alpine belts exhibit sustained or locally increasing frost intensity and frequent transitions through the frost-cracking temperature window. The Wet-Frost Index highlights a progressive spatial contraction of moisture-effective frost conditions, with linear projections to 2050 suggesting that effective frost weathering will become increasingly restricted to high-altitude mountain environments. These findings show that climate warming is redistributing, rather than uniformly suppressing, frost-driven cryospheric processes at the southern margins of Europe.

**Keywords**: frost weathering; freeze-thaw cycles; cryospheric processes; frost cracking window; climate change; cryoclimatic indices.

https://doi.org/10.5194/egusphere-2026-1044
Preprint. Discussion started: 28 May 2026


## 1. Introduction

Frost weathering, also referred to as cryoclasty or freeze–thaw weathering, is a key cryospheric process that contributes to rock breakdown, sediment production, and the long-term evolution of periglacial and temperate landscapes (Deprez et al., 2020). Beyond its geomorphological significance, also plays a critical role in the deterioration of natural stone and construction materials, affecting both modern infrastructure and the preservation of architectural heritage (Jamshidi, 2024). As such, it represents an important interface between atmospheric forcing, cryospheric processes, and surface materials.

Frost weathering is commonly associated with temperature fluctuations around the 0 °C threshold, which induce repeated freezing and thawing of water within rock pores, fractures, and joints. Upon freezing, water expands by approximately 9%, generating stresses that may exceed the tensile strength of the host material and initiate microcracking (Bell, 1992). Repeated freeze–thaw cycles can progressively weaken the rock fabric, ultimately leading to granular disintegration or block detachment (Liu et al., 2015). However, the physical mechanisms governing frost damage are more complex than simple volumetric expansion. The freezing behaviour of pore water depends on pore size, saturation degree, and thermal gradients, meaning that ambient air temperature alone is an imperfect proxy for internal rock conditions (Dash et al., 2006).

Recognising this complexity, numerous studies have proposed cryoclimatic indices aimed at identifying "effective frost" conditions (Walder & Hallet, 1985; Grossi et al., 2007; Brimblecombe et al., 2010; Hu and Hewitt, 2024). These indices typically combine information on the frequency, intensity, and duration of freeze–thaw events, and in some cases incorporate moisture availability to account for hydro-thermal controls on frost cracking. Such approaches are increasingly important in the context of climate change, where warming trends may simultaneously reduce the number of frost days while increasing the frequency of transitions through critical temperature windows.

At the continental scale, previous assessments have identified frost-related decay as a major driver of material degradation and landscape evolution across Europe (Grossi et al., 2007), while climate projections consistently indicate a general decline in frost days in temperate regions under continued warming (IPCC AR6). However, these large-scale patterns often mask strong regional and local variability arising from topography, elevation, land–sea contrasts, and atmospheric circulation. As a result, national and sub-national in a downscaling analyses are essential to capture the spatial heterogeneity of cryospheric processes and to identify zones where frost weathering may persist, intensify, or disappear under future climate conditions.

This study is focused on Spain as a key case study for cryospheric transition zones. Spain provides a particularly valuable natural laboratory for studying frost weathering under climate change. Located at the southern margin of Europe, the Iberian Peninsula spans a wide range of climatic regimes (from humid oceanic and mountainous environments to inland Mediterranean, semiarid, and subtropical conditions) over relatively short spatial distances. Strong altitudinal gradients, complex topography, and pronounced isolation effects generate sharp contrasts in frost frequency, intensity and seasonal persistence. As a result, Spain encompasses both areas where frost weathering remains a dominant cryospheric process and regions where it is already marginal or episodic.

https://doi.org/10.5194/egusphere-2026-1044
Preprint. Discussion started: 28 May 2026


Importantly, many mountainous areas in Spain lie close to the lower thermal limits of sustained frost activity, making them especially sensitive to climate warming (Hales and Roering, 2007). Small changes in minimum temperature or precipitation regime can therefore produce disproportionate shifts in the effectiveness of frost cracking and related geomorphic processes. From a cryospheric perspective, this places Spain within a broader class of mid-latitude transition zones where warming is expected to redistribute frost-driven processes rather than simply eliminate them. Understanding these dynamics is essential for improving process-based interpretations of landscape evolution at the warm margins of the cryosphere.

In this study, we investigate the spatial and temporal dynamics of frost activity across Spain during the period 1993–2022 using daily meteorological data from 84 stations. We analyse maximum and minimum temperatures, thermal oscillations, and precipitation to characterise climatic aggressiveness relevant to frost weathering. Multiple cryoclimatic indices (including frost days, freeze–thaw cycles, intensity thresholds, cumulative frost severity, and wet-frost conditions) are evaluated to assess their sensitivity and suitability for mapping frost-weathering potential. By combining high-resolution climatic data with process-oriented indicators, this work aims to provide a detailed national-scale assessment of how climate change is reshaping cryospheric weathering processes in southwestern Europe.

## 2. Methodology

### 2.1. Network Design and Station Selection

To analyse the climatic drivers governing cryoclasty on rock surfaces, meteorological data were retrieved from the Spanish State Meteorological Agency (AEMET) synoptic and climatological network. Data acquisition was performed via the AEMET Open Data REST API (Representational State Transfer). The study period spans from 1993 to 2022. To objectively assess the influence of daily temperature and precipitation cycles on rock durability, high-resolution daily series were required. Consequently, long-term homogeneous databases were prioritized and subjected to rigorous quality control protocols (Alexandersson & Moberg, 1997).

The selection of observatories was based on three primary criteria:

(i) Climatic Representativeness: Stations were selected to represent the diverse climatic regions of Spain. Classification was based on both the Köppen-Geiger criteria (1991– 2020 reference period; Chazarra et al., 2022) and geographic factors (latitude, longitude, altitude, and aspect), resulting in ten distinct geographic-climatic areas (Fig. 1). Significant climatic diversity in a relatively small area.

(ii) Spatial Density and Distribution: To ensure uniform coverage across the 506,000 km$^2$ study area, the territory was divided into a 1° x 1° latitude/longitude grid (36°00’08’’N–43°47’36’’N and 4°19’29’’E–9°17’46’’W for mainland Spain and the Balearic Islands; 27°38’N–29°25’N and 13°20’W–18°10’W for the Canary Islands). This spatial interpolation method ensures a

https://doi.org/10.5194/egusphere-2026-1044
Preprint. Discussion started: 28 May 2026


high degree of goodness-of-fit (Karl et al., 1994), with each grid cell containing between one and three representative observatories.

(iii) Data Continuity: Preference was given to first-order stations providing complete and coincident long-term series. Where necessary, second-order stations with equivalent representativeness due to their location and proximity were included.

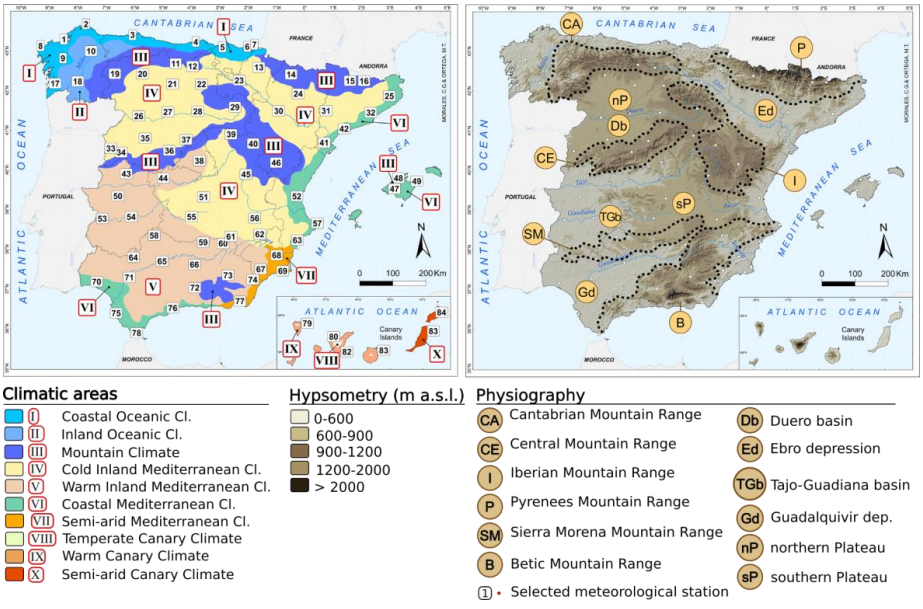


**Figure 1. Left: Climatic areas of Spain and selected meteorological stations. Right: Hypsometric map and main morphoestructural units of Spain. Database sources: IGN (cartographic) and AEMET (meteorological). Meteorological station codes (*: airport): (1) A Coruña; (2) Estaca de Bares; (3) Asturias*; (4) Santander*; (5) Bilbao; (6) Donostia; (7) Hondarribia; (8) Cabo Vilán; (9) Santiago de Compostela*; (10) Lugo*; (11) Cervera de Pisuerga; (12) Polientes; (13) Pamplona*; (14) Jaca; (15) La Seu d'Urgel; (16) La Molina; (17) Vigo*; (18) Ourense; (19) Ponferrada; (20) León; (21) Carrión de los Condes; (22) Burgos*; (23) Logroño; (24) Huesca*; (25) Girona*; (26) Zamora; (27) Valladolid; (28) Aranda de Duero; (29) Soria; (30) Zaragoza*; (31) Lleida; (32) Sabadell*; (33) Saelices El Chico; (34) Ciudad Rodrigo; (35) Salamanca*; (36) Ávila; (37) Segovia; (38) Madrid-Retiro; (39) Sigüenza; (40) Molina de Aragón; (41) Tortosa; (42) Reus*; (43) Plasencia; (44) Talavera de la Reina; (45) Cuenca; (46) Teruel; (47) Palma de Mallorca*; (48) Lluc; (49) Capdepera; (50) Cáceres; (51) Madridejos; (52) València; (53) Badajoz T.R.; (54) Don Benito; (55) Ciudad Real; (56) Albacete*; (57) Xàbia; (58) Hinojosa del Duque; (59) Santa Elena; (60) Arroyo del Ojanco; (61) Villarrodrigo; (62) Hellín; (63) Alicante; (64) Cazalla de la Sierra; (65) Córdoba*; (66) Jaén; (67) Lorca; (68) Murcia; (69) Cartagena; (70) Huelva; (71) Sevilla*; (72) Granada*; (73) Baza; (74) Huércal; (75) Cádiz; (76) Málaga*; (77) Almería*; (78) Tarifa; (79) La Palma*; (80) Izaña; (81) Tenerife Sur*; (82) Gran Canaria*; (83) Fuerteventura*; (84) Lanzarote*.**

https://doi.org/10.5194/egusphere-2026-1044
Preprint. Discussion started: 28 May 2026


From an initial pool of several hundred candidates, 84 stations were selected to provide a robust and reliable sample (Fig. 1). While provincial capitals are well-represented, mountain regions -crucial for cryosphere studies- exhibit a lower density of stations with long-term reliable series. Missing data in these regions were addressed through interpolation procedures.

### 2.2. Data Processing and Quality Control

A homogeneous database was constructed to minimize artificial biases stemming from station relocations, instrumentation changes, or sampling irregularities. Metadata were systematically reviewed to detect outliers, defined as values exceeding $4\sigma^2$ from the mean ($\pm 4\sigma^2/\bar{x}$).

Graphical series comparisons were employed to distinguish instrumental errors from extreme cold events. These low-frequency synoptic events (e.g., cold waves) were preserved, as they are primary drivers of frost-induced rock weathering and determine intense frost parameters. Synoptic validation was performed for the winter semesters using the Climate Forecast System Reanalysis (CFSR) from *Wetterzentrale* (www.wetterzentrale.de). This global model provides 500 hPa geopotential height and surface isobaric maps (0, 6, 12, and 18 UTC) at a 28 km grid resolution, enabling the verification of atmospheric dynamics during extreme episodes.

Missing data (gaps <10%) were filled using stepwise multiple linear regression based on 3–4 neighboring stations within the same climatic area ($R^2 > 0.8$). Small gaps were resolved via linear interpolation. Stations failing to meet these quality thresholds were excluded.

The resulting dataset comprises daily minimum/maximum temperatures, thermal range, and precipitation for 84 stations, totalling 908,850 data points per variable.

Temporal trends and anomalies were analyzed using centered moving averages to smooth variance behavior. Linear regression results obtained via ordinary least squares were subjected to residual analysis to detect and rule out potential autocorrelation. Where necessary, generalized least squares regression was considered. The statistical significance of the observed trends ($p < 0.05$) was primarily assessed using the Mann–Kendall rank correlation test, with Spearman's rank correlation serving as a complementary approach.

For the 30-year projection of the variables, a Holt-type damped trend scheme (Gardner and McKenzie, 1985) was implemented to limit linear extrapolation of historical trends and prevent overestimation. Model parameters were optimized by minimizing the mean squared error (MSE), with the aim of producing a local statistical projection rather than a physically based climate simulation.

The variables used in this study were harmonized with those provided by CMIP6 climate models, specifically including the number of days with sub-zero minimum temperatures, days with above-freezing maximum temperatures, and daily precipitation totals.

https://doi.org/10.5194/egusphere-2026-1044
Preprint. Discussion started: 28 May 2026


### 2.3. Geospatial Analysis and Mapping

Cartographic production was preceded by a geostatistical analysis of each variable to identify spatial dependencies. Using ArcGIS, interpolation models were selected according to the specific behaviour of the data, conditioned by topo-ecological covariates (elevation, distance to the sea, topographic isolation, and latitude), in order to preserve spatial continuity, climatic gradients, and physiographic coherence. The methods applied included inverse distance weighting (IDW), empirical Bayesian kriging (EBK) (using exponential, Whittle, and K-Bessel kernels), and radial basis functions (RBF). Preliminary maps were generated and subsequently validated to calibrate the models prior to the final interpretation of results.

This downscaling approach enabled the generation of spatially continuous surfaces through map algebra and interpolation, which were compared with regionalized projections from the CMIP6 SSP2–4.5 scenario. Model performance was evaluated using error, bias, and spatial agreement metrics against outputs provided by Agencia Estatal de Meteorología (AEMET; Spanish State Meteorological Agency) via its climate change scenario viewer, considering a near-term horizon (“2021–2050”) and multimodel ensemble projections (AEMET et al., 2025).

### 2.4. Cryoclimatic indices and Frost-Weathering Indicators

Frost patterns in Spain over the last 30 years are analysed to evaluate both climatic severity and its specific influence on rock degradation via frost shattering (gelifraction). Within this framework, we define "effective frost" as an event capable of freezing the water stored within the rock’s structural discontinuities (pores, fissures, and joints).

To quantify the frequency and impact of effective frost, we selected parameters that reflect the mechanisms of both superficial and deep-seated frost damage, as well as their synergy with moisture availability (Walder and Hallet, 1985; Grossi et al., 2007; Calle and Van Vliet-Lanoë, 2017; Brimblecombe et al., 2010; Hu and Hewitt, 2024). The selected indicators are:

(i) Annual Frost Days (FD): Total count of days per year where the minimum air temperature ($T_{mn}$) falls below 0°C.

(ii) Freeze-Thaw Cycles (FTC): The number of annual transitions where $T_{mn} < 0$°C and the daily maximum temperature ($T_{mx}$) exceeds 0°C. This includes multi-day transitions where the phase change occurs over successive records.

(iii) Intense Freeze-Thaw Cycles (IFTC): FTC events where $T_{mx} > 1$°C and $T_{mn}$ reaches specific thresholds: –3.5°C, –4.5°C, –6°C, and –10°C. These thresholds identify conditions where the freezing front penetrates deeper into the lithic substrate, causing more significant mechanical stress.

https://doi.org/10.5194/egusphere-2026-1044
Preprint. Discussion started: 28 May 2026


(iv) Frost Intensity Index (FI): Calculated as the square root of the sum of days per year with temperatures below 0°C. This index provides a standardized measure of cumulative cold severity at monthly, seasonal, and annual scales for each station.

(v) Wet-Frost Index (WFI): The number of frost events ($T_{mn}$ < –1°C) preceded by significant moisture availability (daily precipitation > 2 mm within the previous 72 hours). This parameter is critical, as it accounts for the degree of saturation required for ice crystallization to exert sufficient pressure to surpass the rock's tensile strength.

Using these indicators, we analyse frost dynamics across different regimes of intensity, frequency, and duration, identifying spatial patterns and significant temporal trends.

## 3. Results

### 3.1. Spatiotemporal variability of Frost Patterns in Spain

The highest frost intensity is concentrated in alpine and peri-alpine regions, as well as in interior topographic depressions, such as basins, and valleys (Fig. 2). In these environments, annual records frequently exceed 100–110 frost days. Significant frost activity is also observed across the interior of the Iberian Peninsula, particularly in the Duero River basin (Db in Figure 1), followed by the headwaters of the Tajo and Guadiana rivers (TGb in Figure 1). These areas, characterized by a cold inland Mediterranean climate, typically record between 60 and 80 annual frost days.

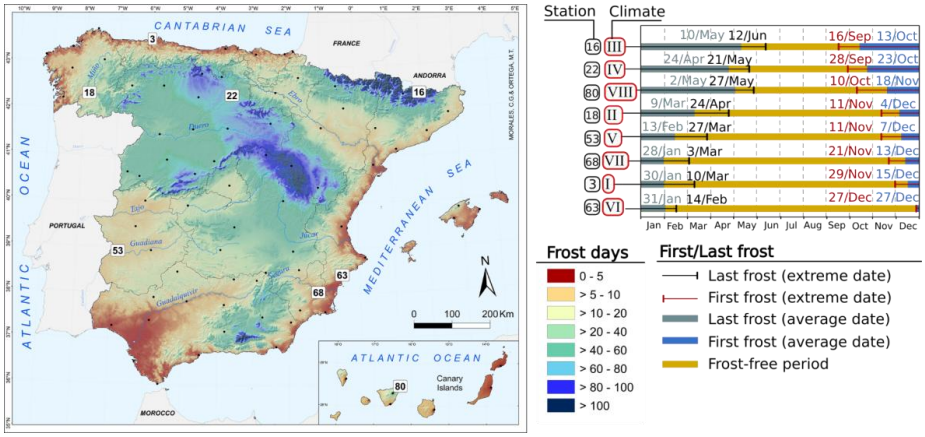


**Figure 2. Spatial variability of frost days in Spain (map; left). Diagram of last/first frosts in eight representative meteorological stations. Station name and climate description in Figure 1.**

Conversely, frost occurrences are marginal along the northern Atlantic coast due to the mitigating effects of the oceanic climate. Similarly, in regions governed by Mediterranean coastal, semi-arid, and Canary

https://doi.org/10.5194/egusphere-2026-1044
Preprint. Discussion started: 28 May 2026


Island (warm and semi-arid) climates, the annual mean generally falls below 10 frost days, with many locations recording fewer than 5 or a total absence of frost events.

The temporal window of frost activity also varies across the Iberian Peninsula. In high-altitude mountainous areas, frost is nearly a year-round phenomenon. In the northern half of Spain, summer frosts are common; for example, at the La Molina station (number 16 in Figure 1), frost events were recorded in July and August in 26.7% and 20% of the analysed years, respectively. The temporal window of frost activity is a critical determinant of its impact on rocks and materials. The duration governs whether a site is permanently exposed or subject to episodic events, directly influencing the frequency of Freeze-Thaw Cycles (FTC).

To define the frost-active season, the average and extreme dates for the First Frost (FF) and Last Frost (LF) events have been computed, alongside the Frost-Free Period (FFP) (Fig. 2), obtaining the sequent results:

- First Frost (FF) Trends: Approximately 19% of observatories (Atlantic and south Mediterranean coasts and low-lying island sectors) do not record FF. In 42.9% of the stations, there is a clear delaying trend, with FF shifting from October to November or December. However, in 20.2% of stations (primarily in the cold Mediterranean climate of the northern plateau (nP in Figure 1), frost tends to appear earlier.
- Last Frost (LF) Trends: LF occurs every year in 54.8% of the observatories. Crucially, 78.6% of stations show a marked trend toward earlier occurrence, with the frost season shortening by 20 to 30 days.

Our data reveal that late (spring) frosts are significantly more frequent than early (autumn) frosts. Over the last 30 years, the first semester recorded twice as many frost days as the second. This indicates that spring is more prone to frost events than autumn, suggesting that the most effective frost-induced rock breakdown occurs between January and April/May.

The Frost-Free Period (FFP) exhibits high spatial variability, ranging from fewer than 150 days in mountain areas to over 300 days in coastal Mediterranean and oceanic climates. Considering extreme dates, the FFP can drop below 100 days in high-risk zones, a parameter essential for assessing the maximum potential for absolute frost-related risk.

### 3.2. Spatiotemporal variability of Cryoclimatic indices

#### 3.2.1. Dynamics of Freeze-Thaw Cycles (FTC) and Frost Days (FD).

The spatial distribution of air-temperature FTCs ($T_{mn} < 0°C$ and $T_{mx} > 0°C$) closely aligns with the annual number of Frost Days (FD). This indicates that sub-zero minima are predominantly followed by positive maxima, a condition that favours significant diurnal thermal oscillations.

FTC frequency is highest in the northern mountain ranges, where cycles exceed 100–110 days per year, and in the northern plateau (nP in Figure 1), averaging 75–85 days. Conversely, FTC incidence is negligible (< 2 days) in oceanic, coastal Mediterranean, and subtropical Canary Island climates (Figs. 3). Over the last

https://doi.org/10.5194/egusphere-2026-1044
Preprint. Discussion started: 28 May 2026


30 years, all observatories exhibit a slight downward trend, which is more pronounced in high-frequency areas where frost intensity is traditionally more severe.

To assess the mechanical stress exerted on the rocks, we analyzed IFTCs using specific intensity thresholds ($T_{mx}$ > 1°C and $T_{mn}$ < -3.5°C, -4.5°C, -6°C, -10°C). These thresholds ensure the phase transition of interstitial water within the rock.

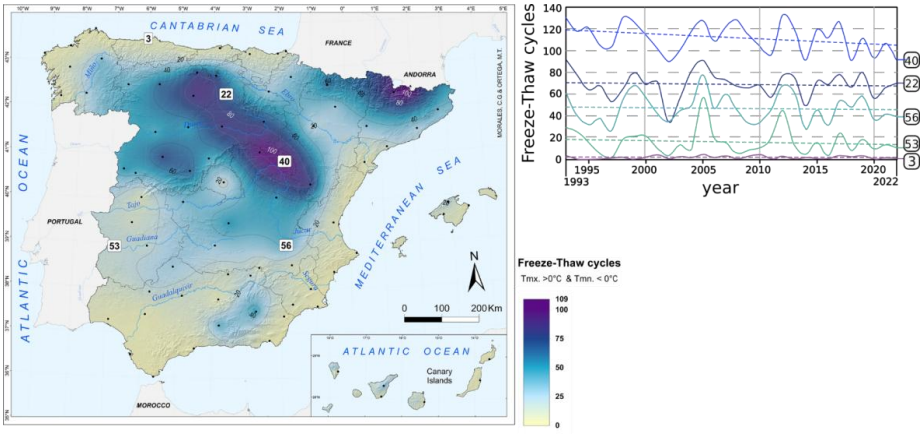


**Figure 3. Spatial distribution of the Freeze-Thaw cycles (left) and temporal evolution from 1993 to 2022 of five representative meteorological stations.**

### 3.2.2. Intense Freeze-Thaw Cycles (IFTC).

Our data show that outside mountain regions, IFTC frequency drops sharply across all climate zones, remaining significant only in the cold inland Mediterranean (Fig. 4). A key observation is that plateau areas (900–1100 m a.s.l.) often exhibit more effective IFTCs than high-altitude peaks. At extreme altitudes, "ice days" (where both $T_{mx}$ and $T_{mn}$ remain below 0°C) prevent the necessary thawing phase, whereas mid-altitude sites fluctuate more frequently across the freezing point. In the context of global warming, while frost episodes are decreasing in temperate zones, an increase in FTCs may occur in previously "permanently frozen" highaltitude regions as rising temperatures push more days into the frost-cracking window (Vyshkvarkova and Sukhonos, 2023).

### 3.3.3. Frost Intensity (FI) Index

The FI index quantifies the cumulative severity and duration of frost events. Mean values range from 0 to 11 (Fig. 5), peaking in the Iberian Mountain range (I in Figure 1, FI > 10). A significant finding is that 32.1% of observatories—primarily in the peri-alpine sectors of the Pyrenees and Cantabrian Mountains (P and CA in Figure 1)—show a positive trend in FI (Fig. 5), suggesting an increase in frost severity in these specific fringes. In contrast, 53.6% of the territory shows a negative trend, forming a diagonal corridor from the SW to the NE (Ebro depression; Ed in Figure 1). Overall, 67.9% of stations exhibit either a decline or stability in FI, confirming a general attenuation of annual frost severity in Spain.

https://doi.org/10.5194/egusphere-2026-1044
Preprint. Discussion started: 28 May 2026


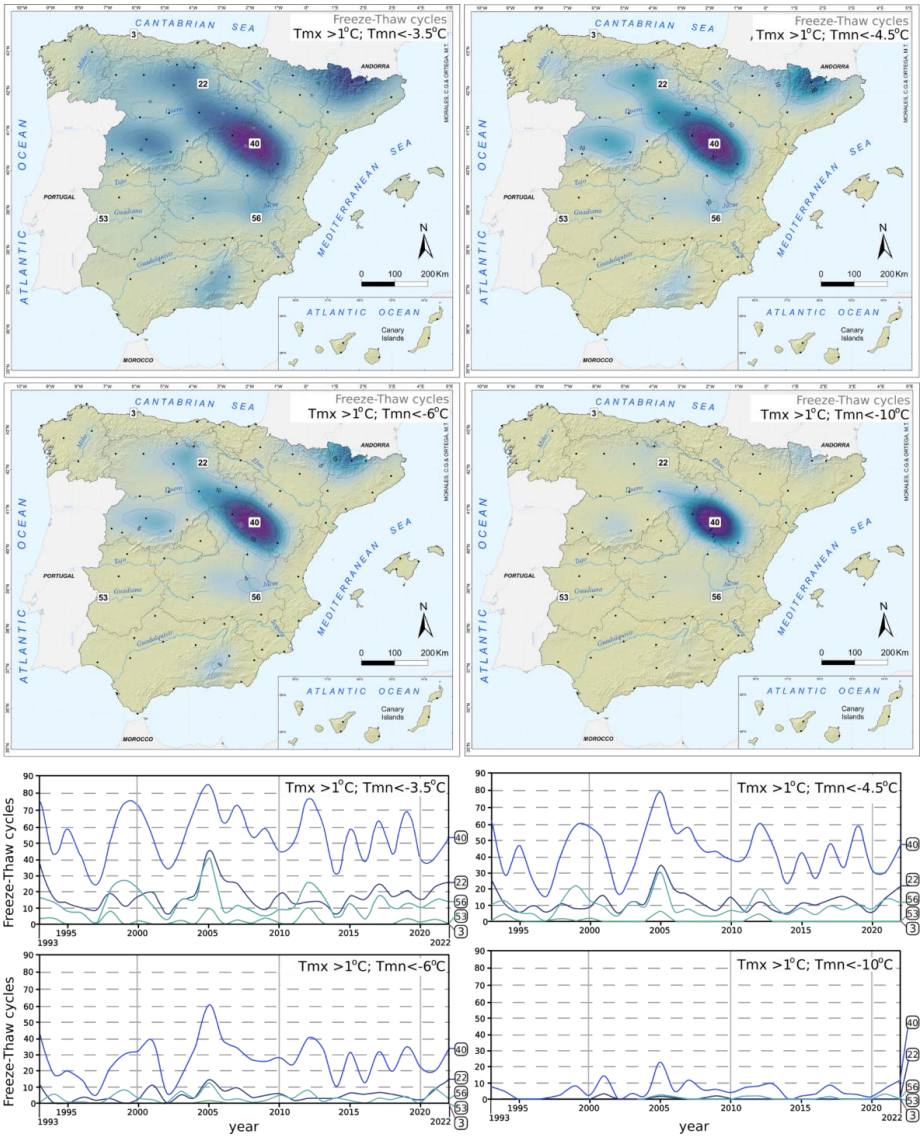


**Figure 4. Spatial distribution of the Intense Freeze-Thaw cycles and temporal evolution from 1993 to 2022 of five representative meteorological stations. Note that the colour scale of the maps has remained fixed even though the number of cycles varies in each map.**

https://doi.org/10.5194/egusphere-2026-1044
Preprint. Discussion started: 28 May 2026


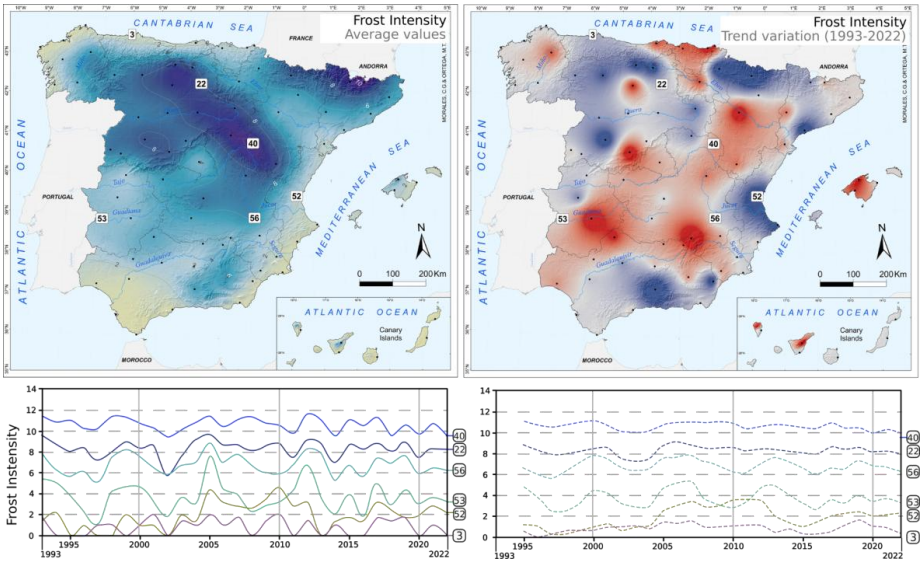


**Figure 5: Geographic distribution of the average values of the Frost Intensity parameter (top left map) and the trend of evolution during the period 1993-2022 (top right map). Lower graphs: evolution of values in the period 1993-2022 of six representative stations represented by their annual values (left graph) and trend of the moving average (right).**

### 3.2.4. Wet-Frost Index (WFI) and Hydro-Thermal Synergy

The WFI (precipitation > 2 mm within 3 days prior to $T_{mn}$ < -1°C) identifies the most effective frost events for rock weathering. The highest values (21–25 annual days) occur in the northern ranges (P, CA and I in Figure 1), where moisture and sub-zero temperatures frequently coincide (Figure 6).

WFI trends show high spatial complexity due to the stochastic nature of precipitation (Kendon et al., 2018) (Figure 6). While 46.4% of stations show a downward trend, 29.8% (including the Pyrenees, Cantabrian and Betic ranges; P and B in Figure 1) show a positive trend. This variability highlights that the WFI is increasingly governed by changes in precipitation patterns rather than temperature alone (Labajo and Piorno, 2001; Ortega and Morales, 2013; Kendon et al. 2018). The higher absolute variations in WFI compared to FI emphasize the erratic behaviour of moisture-dependent weathering processes.

https://doi.org/10.5194/egusphere-2026-1044
Preprint. Discussion started: 28 May 2026


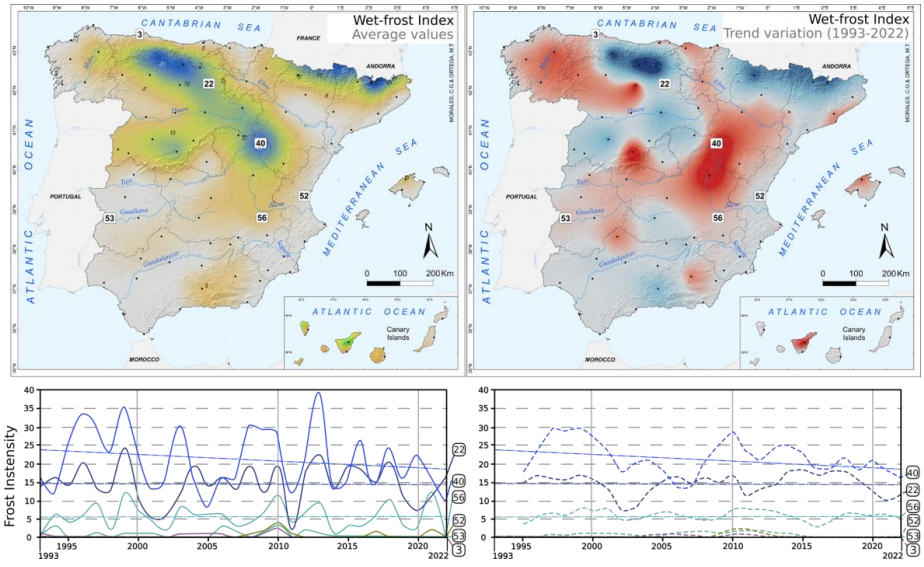


**Figure 6: Geographic distribution of the average values of the Wet-Frost Index (top left map) and the trend of evolution during the period 1993-2022 (top right map). Lower graphs: evolution of values in the period 1993-2022 of six representative stations represented by their annual values (left graph) and trend of the moving average (right). Each curve includes the regression line.**

## 4. Discussion

### 4.1. Atmospheric Dynamics and Synoptic Drivers of Frost in Spain

Two specific synoptic patterns favour the occurrence of frost in Spain, often leading to synchronized extreme events across multiple observatories due to the intensity and depth of the atmospheric situation.

*Radiative Frost (Anticyclonic Ridge):* Most events are associated with a marine Tropical (mT) anticyclonic ridge, often acting as a blocking situation over the Iberian Peninsula. These conditions promote intense nocturnal longwave radiation and cumulative cooling. Such dynamics create significant vertical temperature gradients; for instance, temperatures may reach -6°C at 10 cm above the ground while remaining at 0°C at the standard 150 cm height (García de Pedraza et al., 1977). This favours high diurnal temperature ranges (DTR), which accelerate rock fatigue and mechanical weathering.

*Advective Frost (Arctic/Polar Air Masses):* These are driven by the incursion of marine Arctic (mA) troughs centered over or slightly east of the Peninsula, bringing cold, moist air directly from high latitudes, often accompanied by wind and snowfall in mountain ranges. Alternatively, retrograde flows of continental Polar (cP) air —or "shear lines"— introduce Siberian air masses from the NE. These are typically drier, resulting in less snowfall (Ortega and Morales, 2023). Under these advective conditions, the diurnal cycle is disrupted, and absolute minima can occur at midday.

https://doi.org/10.5194/egusphere-2026-1044
Preprint. Discussion started: 28 May 2026


At a regional scale, we observe departures from these broad synoptic patterns that can locally modulate the overarching conditions across Spain, either exacerbating or attenuating frost events at the local level. For instance, high-elevation basins within the Iberian interior tend to enhance frost frequency throughout the year. This high frequency is driven by nocturnal radiative cooling and the formation of persistent Cold Air Pools (Whiteman et al., 2001), a process frequently documented in the complex topography of the Iberian Peninsula (Conangla et al., 2018). Conversely, frost occurrences remain marginal (fewer than 10 frost days per year) along the northern Atlantic coast due to the moderating influence of the maritime climate.

### 4.2. Geographical variability of freezing mechanisms

The observed spatial distribution of frost effectiveness parameters highlights a fundamental distinction between the two primary physical mechanisms of cryoclasty: volumetric expansion and ice segregation. Traditionally, frost weathering was attributed almost exclusively to the 9% volumetric expansion of water upon freezing within a closed system. This process requires high degrees of saturation and rapid cooling to trap water within the pore network. However, our findings—particularly the significance of the Wet-Frost Index (WFI) and the frequency of cycles within the -3 °C to -8 °C range—suggest that ice segregation can play a differentiated role in the long-term mechanical fatigue of materials in Spain. Moreover, based on the Noah's ARK project and the Walder and Hallet (1985) model, the -4.5°C threshold is particularly critical for the propagation of cracks in saturated rock, while temperatures below -10°C may actually limit further frost-cracking efficiency due to reduced ice-segregation rates.

As proposed by the frost-cracking window model (Hales and Roering, 2007), maximum crack propagation does not necessarily occur at the lowest absolute temperatures, but rather during sustained periods within a specific thermal range that facilitates the migration of unfrozen water toward growing ice lenses. This mechanism, driven by thermodynamic suction, exerts pressures that can far exceed the tensile strength of the rock, even at lower saturation levels than those required for volumetric expansion.

In high-alpine sectors, the prevalence of "ice days" may paradoxically limit this process by "locking" moisture in a frozen state. Conversely, in the identified perimountainous regions , the frequent transitions through the frost-cracking window, coupled with the hydro-thermal synergy captured by the WFI, create an optimal "periglacial engine" (Andersen et al., 2015) for rock breakdown. This distinction is crucial for rock weathering, as it shifts the focus from absolute minimum temperatures to the duration and frequency of sustained, moderate intensity frost events (Draebing et al., 2017). As a consequence, a reduction in total frost days across low- and mid-altitude regions is likely to decrease the overall rate of frost-driven rock disintegration, limiting sediment production in these environments. However, in perimountainous zones where transitions through the frost-cracking window remain frequent or even increase, mechanical weathering efficiency may be enhanced despite overall warming. In these settings, repeated cycling around 0 °C promotes subcritical crack growth and fatigue, accelerating granular disaggregation and block detachment.

Moreover, the projected increase in the intermittency of frost conditions may lead to a shift from continuous to episodic sediment production regimes. Short but intense freeze–thaw periods, particularly when coupled with high moisture availability (as indicated by the Wet-Frost Index), can generate pulses of rock

https://doi.org/10.5194/egusphere-2026-1044
Preprint. Discussion started: 28 May 2026


fragmentation that increase debris supply to slopes (Hales and Roering, 2007). This may, in turn, raise the likelihood of mass movements such as rockfalls, debris flows, and shallow landslides, especially in structurally predisposed terrains. In contrast, in high-alpine areas where warming reduces the occurrence of prolonged ice days, a temporary increase in freeze–thaw cycling may destabilize previously frozen rock masses, enhancing paraglacial adjustment processes.

### 4.3. Observed long-term shifts in frost frequency

To evaluate long-term shifts in frost frequency, we analysed daily records spanning 61 years. Three distinct climatological periods were compared: 1961–1990 (P1), 1981–2010 (P2), and 1993–2022 (P3). Data for the first two intervals were sourced from AEMET (2010), while the most recent period (P3) constitutes the core dataset of this study. A comparative analysis reveals statistically significant downward shifts ($p < 0.05$) in frost occurrence across the Spanish territory (Table 1).

In general, a marked reduction in the number of days with minimum temperatures below 0°C is evident in all observatories when comparing P1 and P3 (Table 1). This progressive decline exceeds a 30–35% variation in several stations (e.g., stations 55, 45, 38, 18, 27 and 30; Figure 1 and Table 1), translating to an absolute decrease of approximately 20 frost days per year. Although other stations show a more moderate decline (below 25% or 10%), the negative trend remains consistent across the network.

Table 1. Evolution of the number of days with minimum temperatures below 0°C during the periods 1961-1980 (P1), 1981-2010 (P2) and 1993-2022 (P3). Variation between P3 and P1 expressed in % and number of days (n). The codes and climatic areas are showed in Figure 1.

| **Station** | | **Climatic area** | **P1** | **P2** | **P3** | **P3 - P1 variation** | |
|---|---|---|---|---|---|---|---|
| **location** | **code** | | | | | **(%)** | **(n)** |
| Albacete (arpt.) | 56 | IV | 63.6 | 52.4 | 46.7 | -26.57 | -16.9 |
| Badajoz T.R. | 53 | V | 21.4 | 18.9 | 15.5 | -25.57 | -5.9 |
| Burgos (arpt.) | 22 | IV | 88.6 | 82.0 | 69.0 | -22.12 | -19.6 |
| Ciudad Real | 55 | IV | 48.6 | 35.4 | 27.9 | -42.59 | -20.7 |
| Cuenca | 45 | IV | 73.7 | 62.0 | 51.0 | -30.80 | -22.7 |
| Granada (arpt.) | 72 | V | 51.8 | 48.8 | 44.9 | -13.32 | -6.9 |
| Huesca (arpt.) | 24 | IV | 38.5 | 34.2 | 28.4 | -26.23 | -10.1 |
| Izaña | 80 | VIII | 63.6 | 53.6 | 45.7 | -28.14 | -17.9 |
| León | 20 | IV | 79.1 | 71.5 | 65.8 | -16.08 | -13.3 |
| Madrid Retiro | 38 | V | 18.7 | 15.7 | 11.3 | -39.57 | -7.4 |
| Molina de Aragón | 40 | III | 121.7 | 121.0 | 113.0 | -7.14 | -8.7 |
| Ourense | 18 | II | 32.4 | 27.3 | 21.8 | -32.71 | -10.6 |
| Pamplona (arpt.) | 13 | III | 45.4 | 39.3 | 33.8 | -25.55 | -11.6 |
| Soria | 29 | IV | 94.0 | 83.8 | 74.6 | -20.63 | -19.4 |
| Valladolid | 27 | IV | 67.0 | 56.2 | 46.6 | -30.45 | -20.4 |
| Zaragoza (arpt.) | 30 | IV | 27.5 | 23.1 | 16.9 | -38.55 | -10.6 |

https://doi.org/10.5194/egusphere-2026-1044
Preprint. Discussion started: 28 May 2026


These findings align with the projected climate trajectories for temperate regions within the current global warming framework, as highlighted by the IPCC Working Group II (Pörtner et al., 2022).

When specifically analysing the record of extreme minimum temperatures across Spain, current minimum temperature data are notably less severe than those observed in previous decades. This reduction in extreme frost events aligns with global trends documented in other temperate regions (Richards & Brimblecombe, 2024). As shown in Table 2, absolute minima in the study period (1993-2022) range from -13.2°C (Ávila; station 36) to -25.2°C (Molina de Aragón; station 40). However, these values remain above the historical absolute records for Spain.

According to AEMET, the absolute minimum for a populated area is -30.0°C (Calamocha-Fuentes Claras, Teruel, 1963), while the record for an uninhabited site is -32.0°C (Lake Estangento, Lleida, 1956). Notably, recent citizen science and regional networks (Noromet) reported a record of 35.8°C at Vega de Liordes (1,872 m a.s.l., León) on January 7, 2021.

Table 2. Minimum temperatures registered in Spain during the 1993-2022 period and absolute minimum values during all the registered period. The codes and climatic areas are showed in Figure 1.

| **Station** | | **Climatic area** | **1993-2022 period** | | **Absolute** | |
|---|---|---|---|---|---|---|
| **location** | **code** | | **T Min** | **Date** | **T Min** | **Date** |
| Molina de Aragón | 40 | III | -25.2°C | 12/01/2021 | -28.2°C | 28/01/1952 |
| Teruel | 46 | III | -21.0°C | 12/01/2021 | -22.0°C | 17/01/1945 |
| Burgos (airp.) | 22 | IV | -17.1°C | 20/12/2021 | -22.0°C | 03/01/1971 |
| Albacete (airp.) | 56 | IV | -17.0°C | 29/01/2006 | -24.0°C | 03/01/1971 |
| La Molina | 16 | III | -15.6°C | 13/02/2018 | -21.4°C | ?/02/1956 |
| León | 20 | IV | -15.0°C | 20/12/2009 | -17.4°C | 13/01/1945 |
| Soria | 29 | IV | -13.6°C | 28/02/2006 | -16.0°C | 01/1940 |
| Ávila | 36 | III | -13.2°C | 01/03/2005 | -20.4°C | 17/01/1945 |

### 4.4. Future Projections: Annual Frost Days and the Wet-Frost Index (WFI)

To provide a future outlook, we generated predictive maps for annual Frost Days (FD) and the Wet-Frost Index (WFI) projected to the year 2050.

Our projections indicate that while frost events will persist, their frequency will undergo a significant reduction across the Iberian Peninsula (Figure 7). The most substantial changes are expected in the hypsometric distribution of frost. By 2050, areas exceeding the 100-day frost threshold will likely be restricted to high-altitude Pyrenean (P) sectors above 2500 m a.s.l. At lower elevations, the frost regime in the Cantabrian (CA) and Iberian (I) systems is projected to shift to an 80–100 day range. In the Central

https://doi.org/10.5194/egusphere-2026-1044
Preprint. Discussion started: 28 May 2026


System (CE), frequencies may drop to 60–80 days, while the Betic range (B) could see a reduction to 40–60 days or fewer in its higher zones.

Simultaneously, the "frost-free" or marginal frost zones (<5 days) are expected to expand significantly, covering all coastal perimeters, major archipelagos, and the primary river basins (Tajo, Guadiana, and Guadalquivir). In the southern half of the Peninsula, a dominant shift toward thresholds below 20 annual days is anticipated.

In stations where frosts are recorded every year, an increase in the frost-free period (FFP) is observed in 82.1% of cases. Specifically: (i) 48.7% will experience a shorter frost season (later First Frost and earlier Last Frost); (ii) 25.6% will show a earlier occurrence of both first and last events; and (iii) 7.7% will see a delayed shift in the entire frost window. Crucially, no observatory shows a contraction of the FFP, confirming a generalized reduction in the window of potential frost-weathering activity.

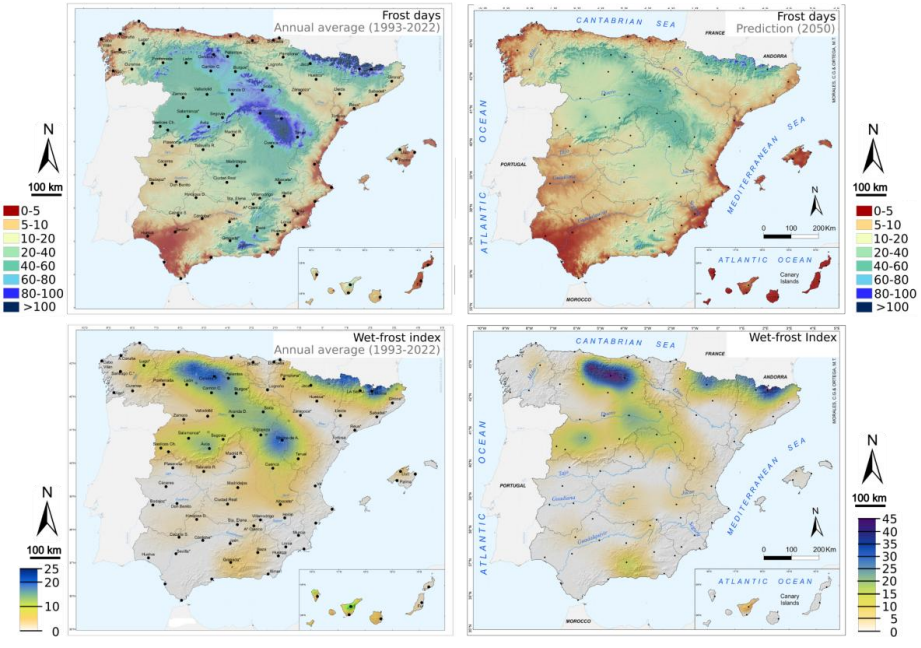


**Figure 7: Geographic distribution of the Frost Days parameter (top) and Wet-frost Index (down). Left maps show the annual average values during the 1993-2022 period and right maps correspond to the predicted distribution for 2050 (according to registered trends during 1993-2022 period).**

Particularly, the Wet-Frost Index (WFI) projection for 2050 reveals a complex spatial pattern (Figure 7) characterized by three main trends: (i) A generalized decrease in hydro-thermal synergy across most of the territory; (ii) A relative stability in current high-intensity hotspots; and (iii) A localized increase in

https://doi.org/10.5194/egusphere-2026-1044
Preprint. Discussion started: 28 May 2026


"unstable" wet-frost days restricted to the northern mountain ranges. This last point is particularly relevant for cryospheric studies. During the 1993–2022 period, stations such as Cervera de Pisuerga (station 11 in Figure 1), Jaca (14), and La Seu d'Urgell (15) showed statistically significant positive trends ($p < 0.01$). However, long-term projections for the WFI must be interpreted with caution. When focusing on the most recent decade (since 2012), the trend directionality becomes erratic, highlighting the stochastic nature of precipitation in the Mediterranean context. Our projection of increased wet-frost frequency in high-altitude, cold environments aligns with recent findings by Richards & Brimblecombe (2024). The critical takeaway is not merely the absolute magnitude of these 2050 estimates, but the spatial contraction of the WFI, which is increasingly confined to alpine enclaves. This trend is driven by two converging factors: the rising minimum temperatures (reducing total frost days) and the increased variability of precipitation, characterized by irregular, high-intensity events separated by prolonged dry spells (Trenberth, 2011; IPCC, 2023).

Our results align broadly with large-scale projects like Noah's Ark and the European Climate Risk Typology. However, these models often rely on administrative divisions (NUTS3) and lowresolution Z-scores, which mask regional singularities. Global models lack the spatial resolution necessary to capture topo-ecological nuances (slope, aspect, cold air pooling) that drive isotropic or anisotropic weathering behaviors. As noted by Richards & Brimblecombe (2024), current global model resolutions are insufficient for detecting the specific climatic micro-processes that cause tangible damage to architectural and lithic materials. Our study demonstrates that national and sub-regional scales are essential to discern the true complexity of climate change impacts on the cryosphere.

In this respect, the results are consistent with the projections adapted for Spain by AEMET (Hernánz et al., 2025). However, it has been observed that the threshold values obtained differ in their magnitude and spatial distribution. In general, a downward trend in the number of days with negative temperatures is evident in both cases. The comparison of modelled historical series with real data conditions the slope on the adjustments and, consequently, the magnitude of the projections. Thus, the models appear to have a tendency to overestimate them, which justifies limiting the comparison to intermediate scenarios (SSP2-4.5) and to "near futures."

Some of the differences in the spatial distribution of the variables also derive from the downscaling method used in this work and the REGbA temperature statistics (Regression with Bias Adjustmen) (Correa Guinea et al., 2023) which, although they correct for the biases of the global models and represent the average trends well, do not capture the complex local patterns conditioned by thermal inversions, the accumulation of cold air in valleys and occasional intense frosts.

## 5. Conclusions

Frost weathering remains an active but increasingly heterogeneous cryospheric process across Spain. Our analysis of five complementary cryoclimatic indicators over the period 1993–2022 reveals a clear spatial structuring of frost effectiveness, strongly controlled by altitude, continentality, and moisture availability.

https://doi.org/10.5194/egusphere-2026-1044
Preprint. Discussion started: 28 May 2026


Alpine and peri-alpine regions emerge as the primary hotspots of effective frost-driven rock breakdown, while coastal Mediterranean, oceanic, and subtropical environments experience negligible frost activity.

At the national scale, a statistically significant decline in frost days, freeze–thaw cycles, and frost season duration is observed at most stations, reflecting the ongoing warming trend documented across southern Europe. The shortening of the frost season (driven by delayed first frost and earlier last frost) reduces the temporal window during which frost weathering can operate, particularly in low- and mid-altitude regions.

However, this general attenuation is not uniform. Perimountainous regions display sustained or locally increasing frost intensity and frequent transitions through the frost-cracking temperature window. These environments exhibit optimal conditions for mechanical fatigue driven by repeated freeze–thaw cycling and ice segregation, in contrast to higher alpine zones where prolonged ice days may limit crack propagation.

The Wet-Frost Index underscores the critical importance of hydro-thermal coupling for effective frost weathering. While temperature controls the overall spatial extent of frost, precipitation variability governs its mechanical efficiency. Our results show a pronounced spatial contraction of wet-frost conditions, increasingly confined to northern mountain ranges, highlighting the growing role of precipitation stochasticity in modulating cryospheric weathering processes.

Linear projections to 2050 indicate that frost activity in Spain will persist but will be progressively restricted to high-altitude environments, with widespread expansion of frost-free or marginal frost conditions elsewhere. This redistribution, rather than a simple reduction, of frost weathering has important implications for sediment production, slope stability, and cryosphere–landscape interactions at the southern margins of Europe, potentially leading to a spatial decoupling between zones of active weathering and zones of sediment transfer and accumulation. More broadly, our study demonstrates the value of high-resolution, national-scale assessments for capturing topoclimatic controls on cryospheric processes that are not resolved by coarse global models.

**Data availability**

The cryoclimatic datasets and high-resolution indices cartographies supporting this study are deposited in the Zenodo repository and are available at: https://doi.org/10.5281/zenodo.18851330. This material is distributed under a Creative Commons Attribution 4.0 International License (CC BY 4.0) (Martinez-Martinez et al., 2026).

**Author contributions**

JMM: Conceptualization, Supervision, Funding acquisition, Writing – original draft, Writing – review & editing. CGM and MTO: Methodology, Investigation, Formal analysis, Visualization, Writing – review & editing.

https://doi.org/10.5194/egusphere-2026-1044
Preprint. Discussion started: 28 May 2026


**Competing interests**

The authors declare that they have no conflict of interest.

**Disclaimer**

Copernicus Publications remains neutral with regard to jurisdictional claims made in the text, published maps, institutional affiliations, or any other geographical representation in this paper. While Copernicus Publications makes every effort to include appropriate place names, the final responsibility lies with the authors. Views expressed in the text are those of the authors and do not necessarily reflect the views of the publisher.

**Acknowledgments**

The authors used AI for language editing and translation of some sentences. The AI tool did not contribute to the scientific content, analysis, or conclusions of the manuscript.

**Financial support**

This work is part of the R&D&I projects PID2020-116896RB-C21 and PID2020-116896RB-C22, funded by MCIN/AEI/10.13039/501100011033 (Spanish Ministry of Science, Innovation and Universities) and the project TEC Heritage-CM (TEC-2024/TEC-39) funded by the Regional Government of Madrid.

**References**

AEMET. (2010). Guía resumida del clima en España. https://www.aemet.es/es/conocermas/recursos_en_linea/publicaciones_y_estudios/publicaciones/detalles/guia_resumida_2010

AEMET, OECC, CSIC. (2025). Climate Change Scenarios Viewer (AdapteCCa). AdapteCCa - Platform on Adaptation to Climate Change in Spain. https://escenarios.adaptecca.es/

Alexandersson, H., Moberg, A. (1997). Homogenization of Swedish temperature data. Part I: homogeneity test for linear trends. International Journal of Climatology, 17 25-34 p. https://doi.org/10.1002/ (SICI) 1097-0088(199701)17:1<25:AID-JOC103>3.0.CO;2-J

Andersen, J. L., Egholm, D. L., Knudsen, M. F., Jansen, J. D., Nielsen, S. B. (2015). The periglacial engine of mountain erosion – Part 1: rates of frost cracking and frost creep. Earth Surface Dynamics, 3(4): 447-462. https://doi.org/10.5194/esurf-3-447-2015

Bell, F.G. (1992): The durability of sandstone as building stone, especially in urban environments. Bulletin – Association of Engineering Geologists, 29(1): 49-60.

Brimblecombe, P., Grossi, C., Harris, I. (2010). Climate change critical to cultural heritage. In: Gökçekus, H., Türker, U., LaMoreaux, J. (eds) Survival and Sustainability. Environmental Earth Sciences. Springer, Berlin, Heidelberg. https://doi.org/10.1007/978-3-540-95991-5_20

Calle, K., Van Den Bossche, N. (2017). Analysis of different frost indexes and their potential to assess frost based on HAM simulations, in ProXIV DBMC 14th International Conference On Durability of Buildings Materials and Components, Ghent, pp. 61–62. http://hdl.handle.net/1854/LU-8525026

Chazarra, A., Lorenzo, B., Romero, R., Moreno, JV. (2022). Evolución de los climas de Köppen en España en el período 1951-2020. Nota técnica 37 de AEMET.

https://doi.org/10.5194/egusphere-2026-1044
Preprint. Discussion started: 28 May 2026


https://www.aemet.es/es/conocermas/recursos_en_linea/publicaciones_y_estudios/publicaciones/detalles/NT_37_AEMET

Conangla, L., Cuxart, J., Jiménez, J., Martínez, D., Miró, J., Tabarelli, D., Zardi, D. (2018): Cold-air pool evolution in a wide Pyrenean valley. International Journal of Climatology, 38(6), 2852-2865. DOI: 10.1002/joc.5467

Correa Guinea, C., Hernanz Lázaro, A., Rodríguez Guisado, E. (2023). Evaluación de métodos de regionalización estadística para la generación de proyecciones climáticas en el marco del PNACC-2 2021-2030. Agencia Estatal de Meteorología. https://doi.org/10.31978/666-23-009-0

Dash, J.G., Rempel, A.W., Wettlaufer, J.S. (2006): The physics of premelted ice and its geophysical consequences. Reviews of Modern Physics, 78(3), 695–741. https://doi.org/10.1103/RevModPhys.78.695

Deprez, M., de Kock, T., De Schutter, G., Cnudde, V. (2020): A review on freeze-thaw action and weathering of rocks. Earth-Science Reviews, 203:103143. https://doi.org/10.1016/J.EARSCIREV.2020.103143

Draebing, D., Haberkorn, A., Krautblatter, M., Kenner, R., Phillips, M. (2017). Thermal and mechanical responses from spatial and temporal snow cover variability in permafrost rock slopes, Teintaelli, Swiss Alps. Permafrost and Periglacial Processes, 28(1): 140-157: DOI: 10.1002/ppp.1921

García de Pedraza, L., Elías, F., Ruiz, L. (1977). Estudio de las heladas en España, S.M.N. Serie A-

76. Madrid. 52 p. https://repositorio.aemet.es/handle/20.500.11765/13695

Gardner, E. S., McKenzie, Ed. (1985). Forecasting Trends in Time Series. Management Science, 31(10), 1237–1246. https://doi.org/10.1287/mnsc.31.10.1237

Grossi, C., Brimblecombe, P., Harris, I. (2007). Predicting long-term freeze-thaw risks on Europe built heritage and archaeological sites in a changing climate. Science of the Total Environment 377. 273-281 p. https://doi.org/10.1016/j.scitotenv.2007.02.014

Hales, T. C., Roering, J. (2007). Climatic controls on frost cracking and implications for the evolution of bedrock landscapes. Journal of Geophysical Research, 112(F2): F02033. https://doi.org/10.1029/2006JF000616

Hernánz, A., Correa, C., Rodríguez, E., Iturbide, M., Gutiérrez, J. M. (2025). Escenarios-PNACC 2024: Nueva colección de escenarios de cambio climático regionalizados del Plan Nacional de Adaptación al Cambio Climático (PNACC). https://escenarios.adaptecca.es/doc/pnacc.pdf

Hu, H. and Hewitt, R.J. (2024): Understanding climate risks to world cultural heritage: a systematic analysis and assessment framework for the case of Spain. Heritage Science, 12: 194.

Jamshidi, A. (2024): Study of building stones durability against the freeze-thaw process: current methods and recommendations for the future. Journal of Building Engineering, 86: 108772.

Karl, Th.R., Knight, R.W., Christy, J.R. (1994). «Global and Hemispheric Temperature Trends: Uncertainties Related to Inadequate Spatial Sampling». Journal of Climate, nº 7, 1144-1163. DOI: 10.1175/1520-0442(1994)007<1144:GAHTTU>2.0.CO;2

Kendon, E.J., Blenkinsop, S., Fowler, H.J. (2018). When will we detect changes in short-duration precipitation extremes? J Clim 31:2945–2964. https://doi.org/10.1175/JCLI-D-17-0435.1

Labajo, J.L., Piorno, A. (2001): Regionalization of precipitation in Castilla and León (Spain). Analysis of its temporal behavior. In Detecting and Modeling Regional Climate Change (BRUNET et al. eds.). Springer-Verlag. Berlín, 163-174.

Liu, Q.S., Huang, S.B., Kang, Y.S., Liu, X.W. (2015): A prediction model for uniaxial compressive strength of deteriorated rocks due to freeze-thaw. Cold Region Sciences and Technologies, 120: 96-107.

https://doi.org/10.5194/egusphere-2026-1044
Preprint. Discussion started: 28 May 2026


Ortega, M.T., Morales, C.G. (2023). Methodology for the historical and synoptic analysis of snows: its application to the region of Castilla y León (Spain). Theor Appl Climatol 151, 1825– 1853 https://link.springer.com/article/10.1007/s00704-022-04336-6

Ortega, M.T., Mortales, C., Labajo, J.L. (2013). Aportaciones sobre cambios en las tendencias de las variables climáticas en la meseta central española. Polígonos. Revista de Geografía. Nº 24. Pp.43-75. ISSN 1132 – 1202

Pötner, H.O., Debra, C., Roberts, C, Adams, H., Adelekan, I., Adler, C., Adrián, R., Aldunce, P., Ali, E., Begum, R.A., Bednar-Friedl, B., Kerr, R.B., Biesbroek, R., Birkmann, J., Bowen, K., Caretta, M.A., Carnicer, J., Castellanos, E., Cheong, T.S., Chow, W., Cissé, G., Clayton, S., Constable, A., et al. (2022). Climate Change. Impacts, Adaptation and Vulnerability. Contribution of working group II to the sixth assessment report of the intergovernmental panel on climate change. Cambridge University Press, Cambridge, UK and New York, NY, USA. 37–118. https://doi.org/10.1017/9781009325844.002

Richards, J., Brimblecombe, P. (2024). Multi‐model ensemble of frost risks across East Asia (1850–2100). Climatic Change 177:68. https://doi.org/10.1007/s10584-024-03723-4

Trenberth, K.E., (2011) Changes in precipitation with climate change. Clim Res 47:123-138. https://doi.org/10.3354/cr00953

Vyshkvarkova, E., Sukhonos, O. (2023). Climate Change Impact on the Cultural Heritage Sites in the European Part of Russia over the Past 60 Years. Climate 11:50. https://doi.org/10.3390/CLI11030050

Walder, J. and Hallet, B. (1985): A theoretical model of the fracture of rock during freezing. GSA Bulletin 96(3):336–346. https://doi.org/10.1130/0016-7606(1985)96<336:ATMOTF>2.0.CO;2

Whiteman, C.D., Zhong, S., Shaw, W.J., Hubbe, J.M., Bian, X., Mittelstadt, J. (2001): Cold Pools in the Columbia Basin. Weather and Forecasting, 16(4): 432-447. doi.org/10.1175/15200434(2001)016<0432:CPITCB>2.0.CO;2